Studies and Simulations of PbPb Collisions at $\sqrt{s_{NN}}$ = 2.76 TeV with the Glauber Monte Carlo Model

Jiankun Zhang[1], Lihong Wang[2], Ning Ni[3], Pengli Wang[4], Xinyun Jiang[5], Yuxin Liu[6, *]

[1] Amador Valley High School, Pleasanton, CA 94566, USA
[2] School of Art and Science, Rutgers University-New Brunswick, New Brunswick, NJ 08901, USA
[3] Eberly College of Science, Pennsylvania State University, University Park, PA 16802, USA
[4] Louis D. Brandeis High School, 13011 Kyle Seale Pkwy, San Antonio, TX 78023, USA
[5] Massachusetts Institute of Technology, Cambridge, MA 02139, USA
[6] Sierra Canyon School, Chatsworth, CA 91326, USA

hebe@neoscholar.com

Abstract. The main purpose of this paper is to simulate nuclear collisions. We review the theoretical background, experimental techniques, and the phenomena presented and provided by the original Glauber model and experiment. Based on the original Glauber model, we change the data and algorithm to test and compare our model with the original results. Then we figure out the spatial eccentricity of quark gluon plasma in different models and analyze the progress in the Glauber model at collider energies.

Keywords: PbPb Collisions, Glauber Monte Carlo Model, nuclear collisions.

1. Introduction

With the progression of physics and the establishment of particle colliders, heavy ion physics is revolutionized. Most of the new particles discovered in recent years are produced by particle collisions at the RHIC and LHC. Furthermore, experiments involving particle collisions provide the theoretical basis for modern nuclear physics. When compared with other subatomic systems in the laboratory, the ultra-relativistic nuclei collision experiments create the highest multiplicities of outgoing particles [1].

The launch of the RHIC makes experiments involving heavy-ion collisions possible. Physicists use these experimental results to simulate, and study matters that exist shortly after the Big Bang in the universe. Specifically, the RHIC uses two independent rings to accelerate and circulate particles in opposite directions, causing them to collide with each other. Then, detectors in the accelerator are used to monitor and collect data from the event [2].

The RHIC typically uses the nuclei of heavy elements, such as those of gold. Due to its physical properties, massive sputtering of particles from gold ions occurs when they collide close to the speed

of light in the RHIC facility. This way, phenomena and data are more easily observed and recorded [2]. For our experiment, we choose to use lead, as, like gold, its nucleus is also densely filled with particles.

Under specific conditions, the collision of heavy nuclei releases large amounts of energy, which usually results in a sharp temperature increase, "melting" the protons and neutrons. Meanwhile, the quarks and gluons, which make up the ions, are liberated. As time passes, the thousands of particles in the area cool off. This closely demonstrates the universe shortly after the Big Bang and achieves one of the main goals of the RHIC [2].

2. Background of the Glauber model

In 1958, Roy Glauber demonstrated various works of his from the past decade, including a model of atomic nuclei. This model creates a solid foundation for many subsequent quantum theories. Meanwhile, the increased reliability of experiments also provides a strong theoretical basis for the experimental results of protons hitting light nuclei, such as deuterons. Relying on Glauber's work, Czyź and Lesniak later observed the dips, positions, and magnitudes of the predicted elastic peaks in 1967. [1]

At its core, the Glauber model describes the total cross sections of beams of hadrons and nuclei during controlled scatterings. This model was later applied to elastic collisions by Czyź and Maximon in 1969, and to inelastic nuclear collisions by Bialas and others. [1]

The miniaturization and universality of computers provide more possibilities for the applications of the Glauber Model. With the revolution of the computer and the increase in computing ability of the personal computer, the Glauber Monte Carlo (GMC) model becomes the default framework, due to it providing simplistic ways to simulate atomic nuclei through realistic programs that generate nucleons. [1]

The GMC allows us to build a simulation in the x-y cartesian coordinate plane, in which two nuclei with a random impact parameter (b) reside. However, the transverse distance between the centroids of each nuclei is utilized, rather than the inelastic nucleon-nucleon cross section, before applying the interaction probabilities to increase the efficiency and reduce the difficulty of simulation. [1]

3. Replicating the Glauber model's original results

For this operation, we use the python programming language to simulate, plot, and analyze data pertaining to different applications of the Glauber Model. To recreate the original Glauber model pertaining to lead 208, we fix the center of one lead nucleus to be the origin of a 3-dimensional cartesian coordinate system. Next, we fix the z coordinate of the center of another lead nucleus to be 0, while randomly choosing 2 numbers between -15 and +15 to be the corresponding x and y coordinates of this second nucleus. This is done as the z direction is assumed to be the direction of travel of the 2 nuclei and restricting the impact to a single 2-dimensional plane maintains the integrity of the experiment, while also simplifying the situation at hand. After the centers of the 2 nuclei have been determined, all 416 nucleons are generated. We take the radius of lead nuclei, 6.62 fm [3] and divide it into 10 concentric shells. We also add 5 additional shells with the same thickness outside of the given radius. For each shell, we take its outer radius, and put that value into equation 1 to approximate the nucleon density of each shell. The nuclear charge density is parameterized by a Fermi distribution [10] with three parameters, nucleon radius R being 6.62 fm, skin depth a being 0.546 fm, and deviation from a spherical shape, w being 0 for lead: [3]

$$\rho(r) = \frac{\rho_0 + \rho_0 w\left(\frac{r}{R}\right)^2}{1 + e^{\frac{r-R}{a}}} \tag{1}$$

When r = R, $\rho(R) = \rho_0$, the normalization constant 0.16. When r goes to infinity, nucleon density is dumped to zero. This function is always valid because the exponential term cannot be negative and cannot be zero after plus one. Once the density is determined, we then multiply it by the volume of each shell to determine the number of nucleons that reside within that region. Random x, y, and z

coordinates from that region, totaling to the number of nucleons, are chosen to represent the position of every nucleon. The computer simulated concept collision diagram is shown in figure 1.

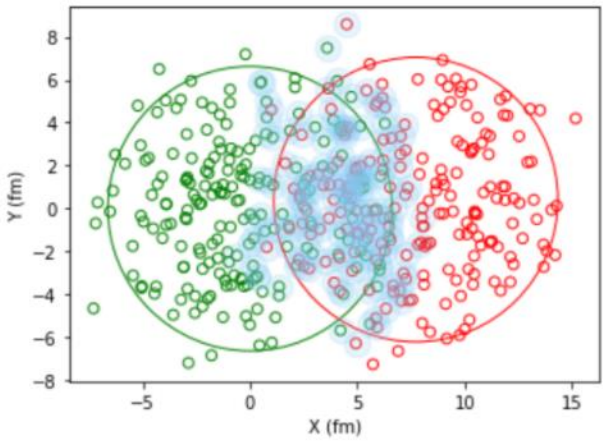

Figure 1. The plot above is a cross-sectional image of an example of our lead nuclei generation process, with the 2 centers being in the same 2-dimensional cartesian coordinate system. Furthermore, 1 nucleus is assumed to be moving into the page, while the other is assumed to be moving out of the page. Lastly, all nucleons highlighted in light blue are assumed to be participant nucleons.

To confirm the validity of our version of the Glauber Model, we measure the total number of participant nucleons, as well as the total number of collisions between nucleons involving lead 208 as a function of the impact parameter. In order to locate the participants, we use the fact that our model simulates collisions conducted at 2.76 TeV, meaning that the inelastic nucleon-nucleon cross sections is approximately 65 millibarns. [2, 4] Thus, the maximum distance D between the centers of 2 nucleons in the x-y plane for them to be considered to have collided can be determined from the following equation: [3]

$$D = \sqrt{\frac{\sigma_{NN}}{\pi}} \tag{2}$$

When solved, D is around 1.44 fm. Therefore, the number of participants equals the number of nucleons that are within 1.44 fm of another nucleon from the other lead nucleus in the x-y plane. [9] Similarly, the total number of collisions can be determined by counting the total number of pairs of nucleons, with one from each nucleus, that are separated by a distance less than 1.44 fm.

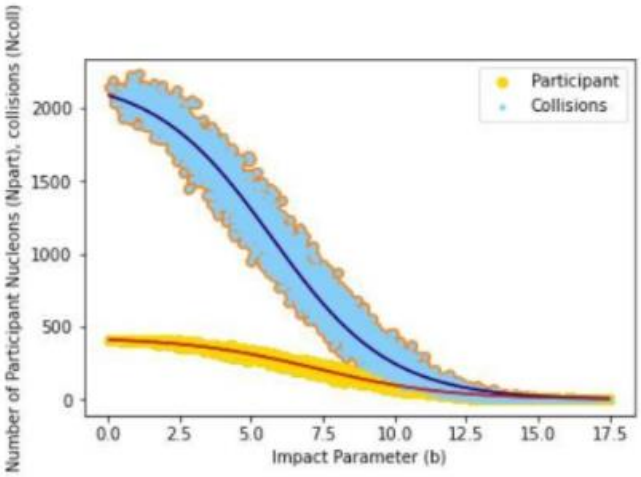

Figure 2. The nucleon participant and collision numbers in lead-lead collisions are plotted against the impact parameter.

In figure 2, both sets of data describing the nucleon participant and collision numbers follow fermi distributions, with N_part approaching 416 and N_coll approaching 2000 as b approaches 0.

4. Applying the Glauber model to constituent quarks

When applying our Glauber Model to the constituent quarks within lead nucleons, we adopt two different approaches. The first approach involves taking every participant nucleon and generating three quarks with random coordinates within a charge radius 0.831 fm [5] from the center of every participant. All of these quarks are then assumed to be participants in the lead-lead collision. The second approach starts by randomly generating 3 quarks inside each one of the 416 nucleons, also by constricting the 3 quarks to within a charge radius of 0.831 fm [5] from the center of the nucleon they make up. Next, the inelastic quark-quark cross section is taken to be one-third that of nucleons, and equation 2 can be applied to all 1248 quarks. When solved, this distance D turns out to be 0.830 fm, which is the upper limit of the separation between the centers of participant quarks, with one from each lead nucleus.

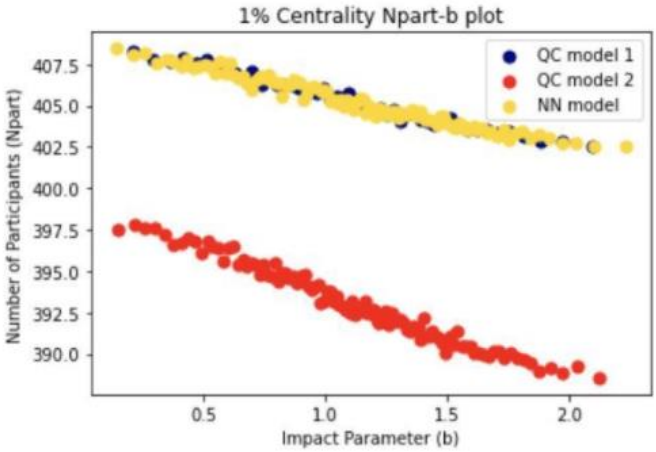

Figure 3. The participant numbers in lead-lead collisions pertaining to our first (QC model 1) and second (QC model 2) quark models, as well as the original nucleon-nucleon model (NN model), are plotted against the impact parameter, with the impact parameter constricted to be of the highest 1% centrality.

For both quark models, participant numbers are based on the baryon number of the colliding particles. Therefore, since the baryon number of quarks is 1/3, the quark participant number equals 1/3 the total number of quarks that are participants.

In figure 3, at small impact parameters, [9] our QC model 1 closely lines up with the NN model. Meanwhile, our QC model 2 has significantly lower values. This is because in our QC model 1, all quarks inside participant nucleons are also considered participants. This, combined with the fact that the 3 constituent quarks of a participant nucleon, together, add to a quark participant number of 1, means that our QC model 1 should be mostly identical to the NN model when it comes to participant numbers. However, with our QC model 2, because the participant status of all 1248 quarks are determined independently from the participant status of the nucleon in which each quark resides, some quarks considered to be participants in our QC model 1 are too far away from the quarks in the other nucleus to be considered a participant here. Therefore, it logically follows that the participant number of our QC model 2 is lower than that of the other 2 models.

In terms of collision numbers at high centralities, 3 quarks of 1 nucleon colliding with the 3 quarks of another nucleon constitutes 1 baryon collision. In terms of our QC model 1, when 2 nucleons collide, all 3 quarks within each participant nucleon are assumed to have collided with all 3 quarks from another participant nucleon, resulting in 9 quark collisions. However, because this is still just 2 nucleons colliding, the baryon collision number is 1. Thus, the ratio between quark collision numbers and baryon collision numbers is taken to be 9:1.

We apply this to both of our quark models by dividing the total number of quark collisions, which are calculated in the same way as the number of nucleon collisions, but using the maximum separation, D, pertaining to quarks, by a factor of 9.

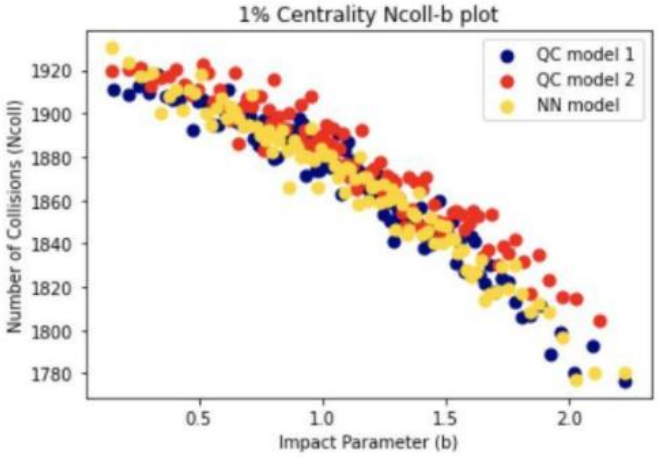

Figure 4. The collision numbers in lead-lead collisions pertaining to our first (QC model 1) and second (QC model 2) quark models, as well as the original nucleon-nucleon model (NN model), are plotted against the impact parameter, with the impact parameter constricted to be of the highest 1% centrality. All three sets of data are based on baryon number. Hence, the collision numbers for our second quark model are divided by three to clearly represent the relation.

In figure 4, all 3 models trend downwards at an increasing rate. Here, our QC model 2 has the most collisions, followed by our QC model 1, and then by the NN model.

5. Eccentricities regular and ultra-central collisions

Experiments at the RHIC and LHC explore phenomena in QCD, most notably the near-perfect fluidity of the quark gluon plasma, a state of hot, dense nuclear matter in which quarks and gluons are not bound into hadrons. [6] A proposed projectile geometry scan that utilizes the unique capabilities of the RHIC [7] can discriminate between hydrodynamical models that couple to the initial geometry, and

initial-state momentum correlation models that do not. Similarly, we adopt the idea in lead-lead collision and change the initial geometry from dominantly circular, to elliptical and triangular configurations, as characterized by the second and third-order spatial eccentricities [11-12] that correspond to ellipticity and triangularity respectively. The nth order of the spatial eccentricities of the system (ε_n), is defined as: [8]

$$\varepsilon_n = \frac{\sqrt{\langle r^2 Cos(n\varphi)\rangle^2 + \langle r^2 Sin(n\varphi)\rangle^2}}{\langle r^2 \rangle} \tag{3}$$

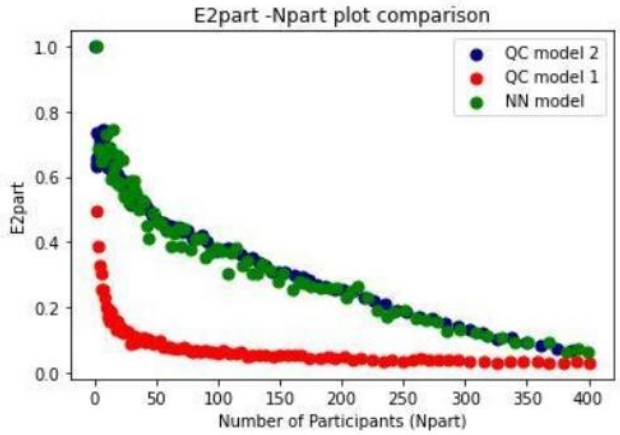

Figure 5. The mean values of the second-order eccentricities in lead-lead collisions pertaining to our first (QC model 1) and second (QC model 2) quark models, as well as the original nucleon-nucleon model (NN model) for each participant number are plotted against the numbers of participants.

In figure 5, the second-order eccentricities of our QC model 1 follows a decreasing exponential trend, while having values significantly less than those of the other 2 models. Meanwhile, our QC model 2, as well as the NN model, follow a decreasing exponential trend on the domain from 0 to 50, and then transition to a decreasing linear trend for the rest of the domain.

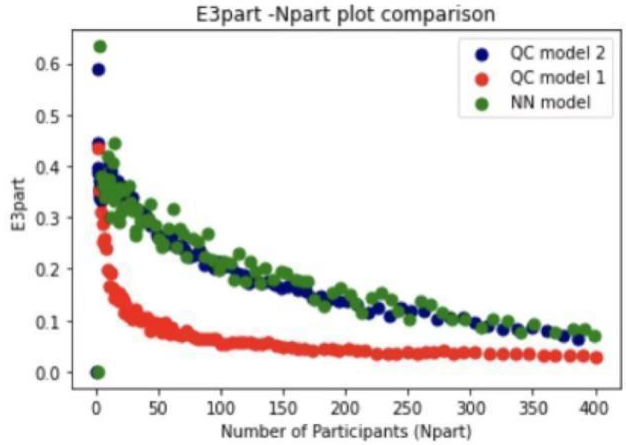

Figure 6. The mean values of the third-order eccentricities in lead-lead collisions pertaining to our first (QC model 1) and second (QC model 2) quark models, as well as the original nucleon-nucleon model (NN model) for each participant number are plotted against the numbers of participants.

In figure 6, all 3 models follow a decreasing exponential trend. However, our QC model 2 consistently has a smaller value than the other 2 models. Meanwhile, the values of our QC model 1 and the NN model are almost entirely identical.

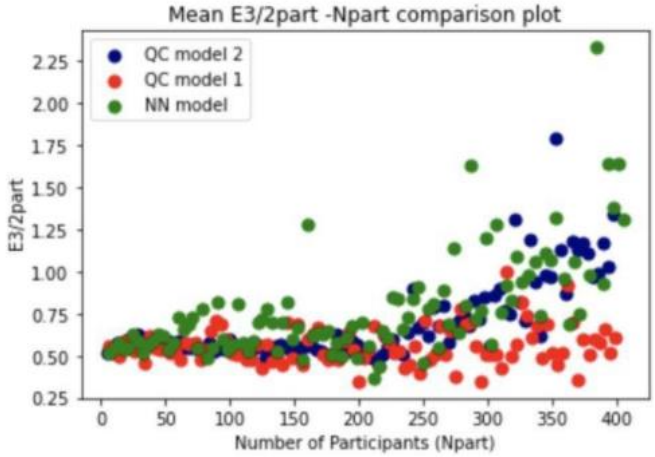

Figure 7. The mean values of the ratio between the second and third-order eccentricities in lead-lead collisions pertaining to our first (QC model 1) and second (QC model 2) quark models, as well as the original nucleon-nucleon model (NN model) for each participant number are plotted against the numbers of participants.

In figure 7, all 3 models follow an increasing, exponential trend. However, the NN model and our QC model 1 start deviating from their exponential trends at around 200 participants. Meanwhile, our QC model 2 follows an exponential progression throughout its domain. Specifically, the NN model has the greatest values, followed by our QC model 2, and then by our QC model 1.

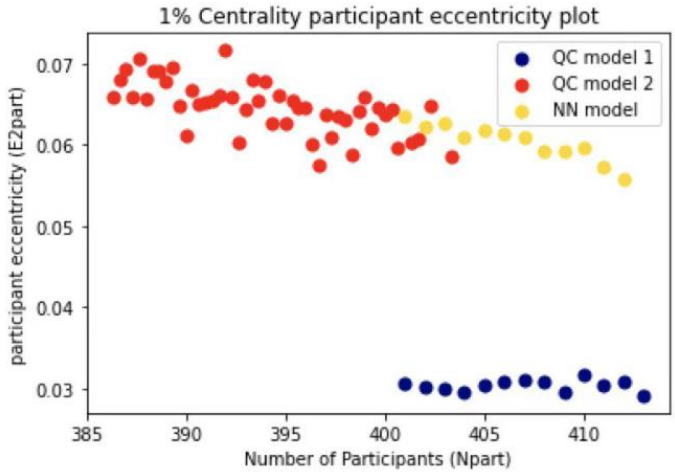

Figure 8. The mean values of the second-order eccentricities in lead-lead collisions pertaining to our first (QC model 1) and second (QC model 2) quark models, as well as the original nucleon-nucleon model (NN model), are plotted against the participant numbers, with the impact parameter constricted to be of the highest 1% centralities.

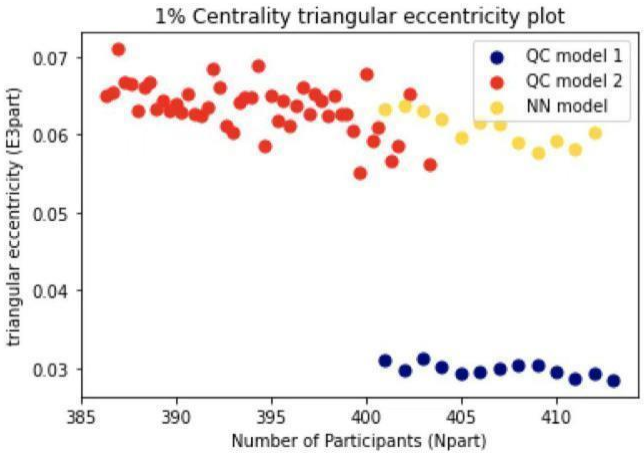

Figure 9. The mean values of the third-order eccentricities in lead-lead collisions pertaining to our first (QC model 1) and second (QC model 2) quark models, as well as the original nucleon-nucleon model (NN model), are plotted against the participant numbers, with the impact parameter constricted to be of the highest 1% centralities.

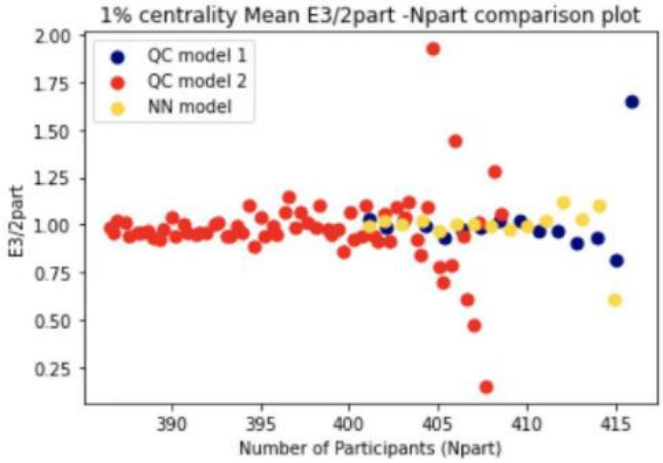

Figure 10. The mean values of the ratio between the second and third-order eccentricities in lead-lead collisions pertaining to our first (QC model 1) and second (QC model 2) quark models, as well as the original nucleon-nucleon model (NN model), are plotted against the participant numbers, with the impact parameter constricted to be of the highest 1% centralities.

In figure 10, all 3 models have data that hover around the same value for most of their domains. However, near their maximum participant numbers, the data become highly erratic.

In figures 8,9, and 10, our QC model 1 and the NN model have similar domains, while our QC model 2 has a domain of a similar size, but with lower participant numbers. This is caused by the participant numbers of our QC model 2 being determined independently from the number of participant nucleons. Hence, some participant quarks in our QC model 1 are not considered participants under our QC model 2.

6. Conclusions

By comparing the results from the three models in ultra-central collisions, our second quark model is evidently, but reasonably different from the nucleon-nucleon model in terms of participant and collision numbers. In addition, our first quark model shows significantly different eccentricity plots from the other two models. It indicates our second quark model simulates lead-lead collision at the quark level better than our first quark model, and the energy $\sqrt{s_{NN}}$ = 2.76 TeV is high enough to allow for collisions between individual quarks from different lead nuclei. Ultra-central collisions make the comparison clear at low impact parameters. Further research is necessary to explore the reasons behind the high uncertainties of the ratio between the third and the second order eccentricities at large participant numbers.

Acknowledgments

We appreciate instructions from Professor Gunther Roland, TA Jack Lin, as well as ideas from the preference list that is given. The authors are listed based on the alphabetical order of first names, without any other determining factor.

References

[1] M. L. Miller, K. Reygers, S. J. Sanders, and P. Steinberg, Annual Review of Nuclear and Particle Science 57, 205-243 (2007).
[2] “The physics of rhic," .
[3] B. Alver, M. Baker, C. Loizides, and P. Steinberg, (2008), arXiv:0805.4411 [nucl-ex].
[4] C. Loizides, J. Kamin, and D. Denterria, Physical Review C 99, 1-23 (2019).
[5] “New measurement fits another piece in the proton radius puzzle," (2020).
[6] I. Arsene et al. (BRAHMS), Nucl. Phys. A 757, 1 (2005), arXiv:nucl-ex/0410020.
[7] J. L. Nagle, A. Adare, S. Beckman, T. Koblesky, J. Orjuela Koop, D. McGlinchey, P. Romatschke, J. Carlson, J. E. Lynn, and M. McCumber, Phys. Rev. Lett. 113, 112301 (2014), arXiv:1312.4565 [nucl-th].
[8] C. Aidala et al. (PHENIX), Nature Phys. 15, 214 (2019), arXiv:1805.02973 [nucl-ex].
[9] S. S. Adler et al. (PHENIX), Phys. Rev. C 89, 044905 (2014), arXiv:1312.6676 [nucl-ex].
[10] M. J. Tannenbaum, Mod. Phys. Lett. A 33, 1830001 (2017), arXiv:1801.06063 [nucl-ex].
[11] J. Jia, (2021), arXiv:2106.08768 [nucl-th].
[12] G. Giacalone, A matter of shape: seeing the deformation of atomic nuclei at high-energy colliders, Ph.D. thesis, U. Paris-Saclay (2020), arXiv:2101.00168 [nucl-th].